ELSEVIER

Thermochimica Acta, 243 (1994) 43–50

thermochimica acta

Physico-chemical characterization and non-isothermal decomposition kinetics of a precursor (polynuclear coordination compound) of manganese ferrite

Oana Carp [a,*], E. Segal [b], Maria Brezeanu [c], Luminita Patron [a], Ruxandra Birjega [d], N. Stanica [a]

[a] *Institute of Physical Chemistry, Splaiul Independentei Nr. 202, sector 6, Bucharest, Romania*
[b] *Department of Physical Chemistry, Faculty of Chemistry, University of Bucharest, Bulevardul Republicii, Nr. 13, Bucharest, Romania*
[c] *Department of Inorganic Chemistry, Faculty of Chemistry, University of Bucharest, Dumbrava Rosie Street, Nr. 23, sector 2, Bucharest, Romania*
[d] *ZECASIN S.A., Chemical Research & Development & Production, Splaiul Independentei, Nr. 202, sector 6, Bucharest, Romania*

(Received 2 June 1993; accepted 16 February 1994)

Abstract

The authors present their results concerning the possibility of using a polynuclear coordination compound, $[Fe^{II}Fe^{III}Mn(C_2O_4)_2(OH)_3(H_2O)_3] \cdot H_2O$, as a source for manganese ferrite. The polynuclear compound synthesized by a forced hydrolysis has been characterized by chemical analysis, electronic and vibrational spectra, X-ray powder diffractometry, magnetic susceptibility measurements and thermal analysis.

This paper also presents a non-isothermal kinetic study of the decomposition steps. The non-isothermal kinetic parameters have been evaluated for the whole (α,t) curve as well as for its significant portions.

Keywords: AAS: Co-ordination compound; Decomposition; Iron compound; IRS; Kinetics; Manganese compound; Non-isothermal; TG; XRPD

1. Introduction

This paper is partially dedicated to topics concerning the elaboration of new methods for mixed oxide syntheses. Many traditional methods such as the reaction

* Corresponding author.

0040-6031/94/$07.00 © 1994 – Elsevier Science B.V. All rights reserved
SSDI 0040-6031(94)01770-H

of oxides in the solid phase, and the thermal decomposition of coprecipitated hydroxides, carbonates or oxalates, have been reported in the literature, but only a few "non-traditional" methods such as the thermolysis of polynuclear coordination compounds [1–3], have been investigated. These compounds are characterized by the presence of ligands with relatively high volatility which decompose rapidly and completely at low temperatures.

In addition to the advantage of a low temperature of synthesis, this procedure has good reproducibility and leads to fine crystallites which confer large specific surface areas to the resulting mixed oxides [4].

The synthesis of manganese ferrite with a definite composition is difficult to perform due to the various oxidation states of manganese ions. According to the literature data, a 1:1 mixture of Fe_2O_3 and MnO_2 oxides can only lead to a single phase product, namely Fe_2MnO_4 at temperatures higher than 1050°C.

Following our research concerning the possibilities of obtaining mixed oxides by the thermal decomposition of polynuclear coordination compounds as precursors, this paper reports the physico-chemical characterization and non-isothermal kinetics decomposition study of a manganese ferrite precursor.

2. Experimental

The polynuclear coordination compound was prepared using a forced hydrolysis procedure [5–7]. The composition of the coordination compound as well as that of its final decomposition product were confirmed by chemical and physico-chemical quantitative analysis: the metal content was determined by atomic absorption spectrophotometry, and the carbon and hydrogen contents were determined using normal combustion method.

The electronic spectra at room temperature were recorded on a Specord M-40, spectrophotometer, in the range 54 000–11 000 cm^{-1}.

The IR spectra were obtained in the range 400–200 cm^{-1} using an infrared Specord type M-80 spectrophotometer.

The crystalline states of the polynuclear coordination compound and of its decomposition products were investigated using a Dron 3 X-ray diffractometer with Co K_α radiation.

For the same substance, the magnetic properties (the magnetic susceptibility and the saturation magnetization) at room temperature were determined using a Faraday balance with $HgCo(SCN)_4$ as calibrant.

The thermal decomposition curves were recorded using a Paulik–Paulik–Erdey Q-1500 D derivatograph in static air atmosphere, with α-Al_2O_3 as the inert reference compound, at heating rates in the range 0.6–10 K min^{-1}.

The values of the non-isothermal kinetic parameters were obtained from the thermogravimetric data using the programs DISCRIM 1 [8] and DISCRIM 2 [9], written in BASIC which allow the most probable mechanism to be selected, using the mean square deviation as the criterion.

Taking into account the possibility of a change in reaction mechanism with conversion, the kinetic analysis of the whole range of conversion ($0 < \alpha < 1$) and in the significant ranges of conversion have been analysed. The intervals $0 < \alpha < \alpha_{ip}$ and $\alpha_{ip} < \alpha < 1$, where the subscript ip indicates inflection points of the TG curve, have been considered. For the TG curves on which an induction period was apparent, non-isothermal kinetic parameters have also been evaluated.

3. Results and discussion

The polynuclear coordination compound was synthesized by hydrolysis of the simple salts, $FeC_2O_4 \cdot 2H_2O$ and $Mn(CH_3COO)_2 \cdot H_2O$. The solution containing the starting materials was kept for some hours at boiling temperature. The final product of the hydrolytic decomposition is a polynuclear coordination compound with the molecular formula $[Fe^{II}Fe^{III}Mn(C_2O_4)_2(OH)_3(H_2O)_3] \cdot H_2O$.

Details of the powder synthesis by this method have been given elsewhere [10].

Information concerning the stereochemistry of the metallic ions was obtained from the electronic spectra. The band positions and assignments [11] are listed in Table 1. From these experimental data, the following conclusions have been inferred: the iron ions (in either oxidation state +2 or +3) exhibit an octahedral geometry with a coordination number of 6, and the manganese ions are in a tetrahedral geometry with a coordination number of 4.

The use of IR spectroscopy to obtain information on the functions of the oxalate anions, is based mainly on the fact that the vibrational modes of the oxalate anions influence the position and, respectively, the number of the absorption bands. The position of the band maxima assigned to the vibrational modes of the oxalate in the polynuclear compound $[Fe^{II}Fe^{III}Mn(C_2O_4)_2(OH)_3(H_2O)_3] \cdot H_2O$ are listed in Table 2.

The positions of these bands are very close to those obtained for $Na_2C_2O_4$ and $FeC_2O_4 \cdot 2H_2O$, also given in the same table. This indicates that oxalate anions in the polynuclear coordination compound have the same function as in $FeC_2O_4 \cdot 2H_2O$, namely double bridged between two metallic ions. Moreover, the

Table 1
d–d Electronic transitions of the metal ion present in the polynuclear coordination compound

Fe(II)		Fe(III)		Mn(II)	
Band position/ cm^{-1}	Assignment	Band position/ cm^{-1}	Assignment	Band position/ cm^{-1}	Assignment
11000	$^5T_{2g} \rightarrow {}^5E_g$	25000	$^6A_{1g} \rightarrow {}^4E_g$	25000	$^6A_1 \rightarrow {}^4T_2$
		18000	$^6A_{1g} \rightarrow {}^4T_{2g}$	20800	$^6A_1 \rightarrow {}^4T_2$
		15000			
		11000	$^6A_{1g} \rightarrow {}^4T_{1g}$		

Table 2
Vibrational modes of oxalate anions (cm^{-1})

$Na_2C_2O_4$	$FeC_2O_4 \cdot 2H_2O$	$[Fe^{II}Fe^{III}Mn(C_2O_4)_2(OH)_3(H_2O)_3] \cdot H_2O$	Assignment
	3340s	3400s	$\nu(H_2O)$
1664[a]	–	–	$\nu_a(O-C-O)$
1640vs	1638vs	1640s	$\nu_s(O-C-O)$
1485, 1450[a]	–	–	
1335s	1360s	1370s	
770sh	825s	820s	$\delta(O-C-O)$
774s			
520s	500s	500s	$\delta(O-C-O)$

Key: sh, shoulder; vs, very strong; s, strong. [a]Raman spectrum of $H_2C_2O_4 \cdot H_2O$ [12].

character of the C–O linkages, despite interactions with metallic ions is not strongly modified in comparison with that of $C_2O_4^{2-}$. In consequence, the tetradentate oxalate anions preserve their planar structure.

The presence of the same hydrogen bonding is demonstrated by a large band in the 3500–3000 cm^{-1} range (with the maximum at 3400 cm^{-1}).

Taking into account all these experimental data, the most probable structural formulation of this polynuclear compound is suggested in Fig. 1.

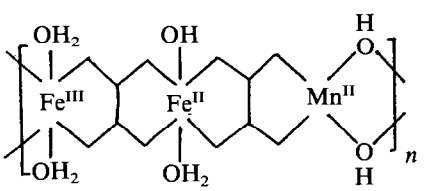

Fig. 1. The suggested structure for $[Fe^{II}Fe^{III}Mn(C_2O_4)_2(OH)_3(H_2O)_3] \cdot H_2O$ (is $C_2O_4^{2-}$).

The magnetic properties of this compound show a paramagnetism, with $\mu_{exp} = 7.02$ BM. This magnetic moment value, lower than that obtained by summing the magnetic moments of the paramagnetic metallic ions, indicates antiferromagnetic interactions, which are generally present in such polynuclear coordination compounds.

As shown by the X-ray powder diffractogram, the polynuclear coordination compound $[Fe^{II}Fe^{III}Mn(C_2O_4)_2(OH)_3(H_2O)_3] \cdot H_2O$ exhibits a crystalline monoclinic lattice isomorphous with that of $FeC_2O_4 \cdot 2H_2O$, which was used as a starting material. Table 3 lists the values of the interplanar distances d and their relative intensities corresponding to the diffraction lines of these two compounds. The Miller indices are also listed. The crystallite size for the most intense line of the polynuclear coordination compound, calculated using Sherrer's formula [13], is $l = 450$ Å.

Table 3
X-ray powder diffraction data

Number of the line	(hkl)	$FeC_2O_4 \cdot 2H_2O$ (ASTM 23-293)		$[Fe^{II}Fe^{III}Mn(C_2O_4)_2(OH)_3(H_2O)_3] \cdot H_2O$	
		d/Å	Relative intensity	d/Å	Relative intensity
1	011	4.80	100	4.803	100
2	200	4.70	65	4.695	83
3	$\bar{2}02$	3.880	25	3.905	9
4	$\bar{1}12$	3.629	20	3.686	10
5	$\bar{2}11$	3.597	20	3.618	12
6	211	3.172	4	3.173	5
7	202	3.004	50	2.994	85
8	020	2.778	4	2.792	4
9				2.705	17
10	$\bar{2}13$	2.654	30	2.670	11.5
11	$\bar{3}12$	2.634	16	2.657	9
12	$\bar{1}21$	2.616	25	2.646	9
13	$\bar{2}04$	2.396	3	2.390	4
14	$\bar{4}02$	2.335	3	2.368	4.5
15	411	2.224	3	2.226	2
16	213	2.190	4	2.183	4
17	$\bar{1}23$	2.122	9	2.146	3
18	$\bar{3}21$	2.106	8	2.103	2
19	$\bar{3}14$	2.037	7	2.040	3
20	$\bar{4}13$	2.021	14	2.012	7
21	123	1.980	3	2.007	6
22	204	1.949	11	1.945	12
23	402	1.929	9	1.927	11
24	$\bar{3}23$	1.893	15	1.894	4
25	$\bar{2}15$	1.847	2	1.843	10
26	$\bar{5}12$	1.816	21	1.822	10
27	420	1.795	4	1.798	3
28	510	1.779	2	1.780	1
29	$\bar{1}32$	1.727	3	1.730	9
30	132	1.683	2	1.693	10

According to the derivatographic data, the polynuclear coordination compound undergoes the following decomposition steps in the range 20–300°C

$$[Fe^{II}Fe^{III}Mn(C_2O_4)_2(OH)_3(H_2O)_3] \cdot H_2O(s) \rightarrow [Fe^{II}Fe^{III}Mn(C_2O_4)_2(OH)_3(H_2O)_3](s) + H_2O(g) \quad (1)$$

$$[Fe^{II}Fe^{III}Mn(C_2O_4)_2(OH)_3(H_2O)_3](s) \rightarrow [Fe^{II}Fe^{III}Mn(C_2O_4)_2(OH)_3](s) + 3H_2O(g) \quad (2)$$

$$[Fe^{II}Fe^{III}Mn(C_2O_4)_2(OH)_3](s) \rightarrow [Fe^{II}Fe^{III}Mn(CO_3)_2O_{3/2}(s) + 2CO(g) + 3/2H_2O \quad (3)$$

$$[Fe^{II}Fe^{III}Mn(CO_3)_2O_{3/2}(s) \rightarrow Fe_2MnO_4(s) + 2CO(g) \quad (4)$$

The experimental total weight loss recorded from the TG data is 50.25%, in comparison with the theoretical value of 50.42%.

The diffractograms of the decomposition end products show a mixture of simple oxides (MnO, α-Fe_2O_3, Fe_3O_4) and manganese ferrite. Performing a cell calculation, as if there were a single phase, for a calcination temperature $T = 400°C$, $a_0 = 8.423$ Å, and for a calcination temperature $T = 450°C$, $a_0 = 8.448$ Å. These values, lower than that for the manganese ferrite ($a_0 = 8.499$ Å) are evidence for the presence of magnetite ($a_0 = 8.396$ Å).

According to the magnetic measurements (Table 4), the oxides exhibit ferrimagnetic properties.

Table 4
Magnetic data at room temperature of the calcination products

Thermal treatment	$\chi_g \times 10^3/(cm^3\ g^{-1})$	$\sigma_s/(emu\ g^{-1})$
3 h at 300°C, slow cooling	2.241	20.302
3 h at 400°C, slow cooling	2.164	19.909
3 h at 450°C, slow cooling	2.664	24.343

Table 5
Non-isothermal kinetic parameter values for the range $0 < \alpha < 1$, $\beta = 2.5\ K\ min^{-1}$

Range/°C[a]	T_{max}[b] °C	Computation program	$f(a)$	A/s^{-1}	E/kcal mol^{-1}	$k \times 10^3/s^{-1}$	Mean square deviation
Reaction (1)							
105–130	116	DISCRIM 2	Contracting sphere	3.20 $\times 10^9$	18.70	97.7[c]	0.37
		DISCRIM 1	$(1-\alpha)^n$ $n = 0.70$	0.90 $\times 10^9$	17.85	85.1[c]	0.50
Reaction (2)							
130–185.5	165	DISCRIM 2	Contracting sphere	1.08 $\times 10^9$	19.40	111.2[d]	2.82
		DISCRIM 1	$(1-\alpha)^n$ $n = 0.70$	0.92 $\times 10^9$	18.95	161.5[d]	2.83
Reaction (3)							
191–232	227	DISCRIM 2	Contracting sphere	9.24 $\times 10^{24}$	58.78	–	7.64
		DISCRIM 1	$(1-\alpha)^n$ $n = 0.62$	1.70 $\times 10^{24}$	55.50	–	9.93
Reaction (4)							
232–262			Contracting cylinder	1.50 $\times 10^4$	11.86	–	0.67
		DISCRIM 2	Contracting sphere	1.50 $\times 10^{11}$	28.60	–	0.69
		DISCRIM 1	–	–	–	–	–

[a]T_i, initial temperature of the reaction; T_f, final temperature of the reaction. [b]T_{max}, temperature of the inflection points where the reaction rate reaches its maximum value. [c]Calculated for $T = 390$ K. [d]Calculated for $T = 426$ K.

Table 6
Non-isothermal kinetic parameters for various portions of the curve (α,t), $\beta = 2.5$ K min^{-1}

Conversion range	Range/°C	$f(\alpha)$	A/s^{-1}	E/kcal mol^{-1}	Mean square deviation
Reaction (1)					
$0-\alpha_{ip}$ (0–0.3696)	105–116	Contracting sphere	2.40×10^{9}	18.49	18.49
$\alpha_{ip}-1$ (0.3696–1)	116–130	Contracting cylinder	8.42×10^{8}	17.80	16.05
		Contracting sphere	1.70×10^{9}	18.60	17.32
Reaction (2)					
$0-\alpha_{ip}$ (0–0.5452)	130–165	Contracting cylinder	7.07×10^{7}	17.75	4.91
		Contracting sphere	4.97×10^{6}	15.64	5.69
$\alpha_{ip}-1$ (0.5452–1)	165–185.5	Contracting cylinder	3.18×10^{2}	6.83	1.14
Induction period (0–0.2427)	130–150	Power law $(1/n)^{n-1}$ $n = 3/2$	5.43×10^{26}	48.33	1.52
Acceleratory period (0.2427–0.5452)	150–165	Contracting sphere	4.58×10^{8}	19.36	6.68
Reaction (3)					
$0-\alpha_{ip}$ (0–0.6788)	191–227	Contracting sphere	6.72×10^{24}	58.35	2.50
$\alpha_{ip}-1$ (0.6788–1)	227–232	Contracting sphere	2.40×10^{23}	56.59	7.32
Induction period (0–0.1097)	192–212	Power law $(1/n)\alpha^{n-1}$ $n = 3/2$	2.95×10^{28}	64.95	6.98
Acceleratory period (0.1097–0.6788)	200.5–227	Contracting sphere	9.72×10^{24}	59.72	2.48

For the kinetic studies five different heating rates were used: 10, 5, 2.5, 1.25, and 0.6 K min^{-1}. For each reaction step, the temperature intervals of its occurrence, the kinetically workable conversion intervals, the most probable mechanism, the non-isothermal kinetic parameters and the mean square deviations were determined. The sample weights used in the non-isothermal kinetic studies were 0.100 ± 10 g%.

Tables 5 and 6 give the results obtained for the heating rate $\beta = 2.5$ K min^{-1} only. Table 5 lists the values of the non-isothermal kinetic parameters corresponding to the (α,t) curve, for all the values of the degree of conversion. The rate constants calculated by the Arrhenius equation for a temperature located in the range of occurrence of reactions (1) and (2) are also listed. Table 6 lists the values of the non-isothermal kinetic parameters for significant portions of the (α,t) curves.

An examination of these two tables reveals the following.

(i) The reactions take place according to a contracting geometry mechanism (contracting sphere and cylinder). The two models have comparable probabilities in the same cases.

(ii) The contracting geometry mechanism is preserved in the conversion ranges $0 < \alpha < \alpha_{ip}$, $\alpha_{ip} < \alpha < 1$, and during the acceleratory period.

(iii) The induction period, when detected, is described by a power law, $\alpha^n = kt$ with $n = 3/2$.

(iv) For reaction (4), the kinetic analysis was not extended over a significant portion of the (α,t) curve, due to the difficulties in locating exactly the maximum of the DTG curve, which spreads over a large temperature range.

4. Conclusions

The polynuclear coordination compound $[Fe^{II}Fe^{III}Mn(C_2O_4)_2(OH)_3(H_2O)_3] \cdot H_2O$ was prepared and characterized and its thermal stability was investigated. The compound decomposes to a mixture of simple oxides (MnO, α-Fe_2O_3 and probably F_3O_4) and manganese ferrite (Fe_2MnO_4).

Using discrimination methods, the most probable mechanism and the non-isothermal kinetic parameters for $0 < \alpha < 1$ have been determined.

For reactions (1), (2) and (3), the non-isothermal kinetic parameters were determined for significant portions of the (α,t) curve. Over the whole range of conversion ($0 < \alpha < 1$), as well as on significant portions of the conversion curve, the reaction investigated can best be described by a contracting geometry mechanism.

The most probable kinetic law describing the induction period is $\alpha^n = kt$ with $n = 3/2$.

References

[1] J. Paris and R. Paris, Bull. Chem. Fr., 4 (1965) 1138.
[2] I. Ilie, M. Brezeanu and E. Segal, Thermochim. Acta, 94 (1985) 393.
[3] P. G. Schullerus, L. Patron, S. Plostinaru, A. Contescu and E. Segal, Thermochim. Acta, 153 (1989) 263.
[4] M. Brezeanu, L. Patron and M. Andruh, Polynuclear Coordination Compounds and their Application, Ed. Academia, Bucharest, 1986.
[5] S. Hamada and E. Metyivec, J. Chem. Soc. Faraday Trans., 78 (1982) 2147.
[6] S. Hamada, K. Bando and J. Kudo, Bull. Chem. Soc. Jpn., 59 (1986) 2063.
[7] S. Hamada, S. Diizaki and J. Kudo, Bull. Chem. Soc. Jpn., 59 (1986) 3443.
[8] T. Coseac and E. Segal, Thermochim. Acta, 149 (1989) 189.
[9] O. Carp and E. Segal, Thermochim. Acta, 185 (1991) 111.
[10] M. Brezeanu, L. Patron, O. Carp, E. Cristurean, A. Antoniu, M Andruh, A. Gheorghe and N. Stanica, Rev. Roum. Chim., 11 (1993) 1291.
[11] F. A. Cotton and G. Wilkinson, Advanced Inoreganic Chemistry, 2nd edn., Interscience, New York, 1966.
[12] K.L. Scott, R. Weighard and A.G. Sykes, Inorg. Chem., 12 (1973) 655.
[13] H. Klug and L.E. Alexander, X-Ray Diffraction Procedure, John Wiley, New York, 1962, p. 461.